

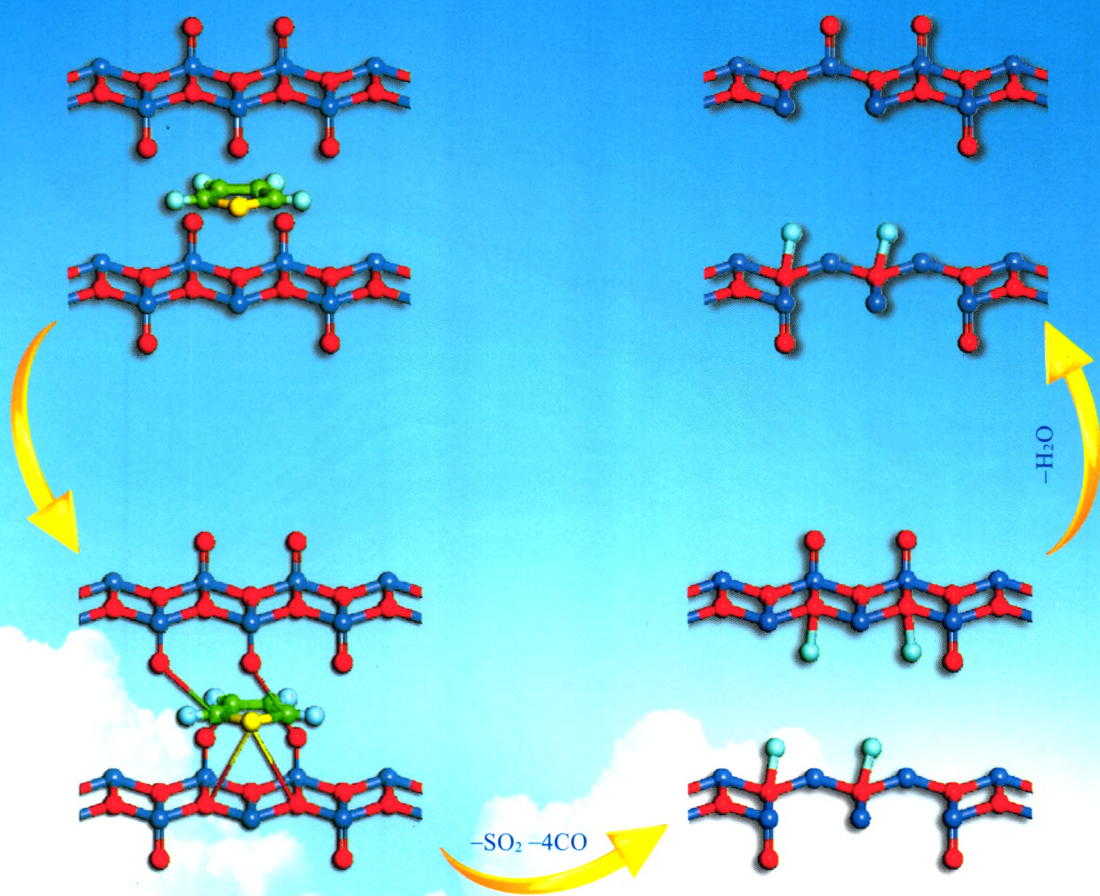


中文核心期刊 Ei核心期刊  
本刊被Ei Compendex,CA,AJ,CBST,Scopus等  
国际重要检索数据库收录

ISSN 1001-8719  
CN 11-2129/TE  
CODEN SXSHEY

# 石油学报 (石油加工)

## ACTA PETROLEI SINICA (PETROLEUM PROCESSING SECTION)



ISSN 1001-8719



万方数据

中国石油学会主办  
石油化工科学研究院 承办

2013

3  
Vol.29

# 石 油 学 报

(石油加工)

第 29 卷 第 3 期 2013 年 6 月

## 目 次

### 研究报告

噻吩脱硫过程中钒氧化物晶格氧的作用*	王 鹏 任 奎 田辉平 龙 军(369)
柴油加氢改质过程烃类反应与十六烷值的关系	张永奎 胡志海 刘晓欣 聂 红(376)
氨基酸功能化杂多酸盐的制备及其在无溶剂条件下催化正十二醇与乙酸酯化反应性能	刘 静 黄小文 赵小平 刘秀梅 颜佩芳 王 畅 高艳安(383)
含铜类水滑石高选择性催化氧化甘油	刘献锋 张 方 王晓丽 丁克强 王 芳 刘俊华 宋晓波 吴功德(390)
催化加氢改性生物质油轻质组分	胡恩柱 徐玉福 李文东 刘天霞 胡献国(398)
新型酚酰胺抗氧化剂 AO-BIO 的合成及在生物柴油中的应用	刘金胜 蔺建民 张建荣 张永光(404)
汽油催化裂解制丙烯集总动力学模型 II. 动力学模型分析	吕庐峰 李 博 何金龙 侯栓弟(409)
生物柴油组分在铁表面吸附的分子动力学模拟	罗 辉 范维玉 李 阳 南国枝(416)
固定床反应器中生物油水溶性组分热解反应动力学	刘少敏 陈明强 胡青松 杨忠连 李 峰 汪 娟 王 君(422)
氢气还原硝酸盐的理论研究	李 倩 郭大为 周 涵(427)
采用白土树脂串联方案净化环丁砜贫液	韩 东 张纪梅 李明玉 魏 君(433)
流化床中造纸黑液催化石油焦气化特性	于德平 张玉明 杨运泉 高士秋 许光文(438)
无硫磷啉酮胺多效润滑油添加剂的性能	欧阳平 陈国需 张贤明(447)
PLS-XRD 快速测量 S Zorb 再生剂中尖晶石含量	付 颖 张 欣 邹 亢 徐广通(453)
委内瑞拉稠油沥青质的 XPS 研究	李 传 王继乾 隋李涛 崔 敏 邓文安(459)
新型抗高温抗盐钻井液增黏剂 PADA 的制备与性能	闫丽丽 孙金声 王建华 王成彪 许 博 杨泽星(464)
聚丙烯酸钠树脂孔径调节及油水选择吸附平衡控制	吴 云 张贤明 陈 彬 陈国需(470)

### 研究报道

环烷烃催化裂解生成乙烯和丙烯反应探析	于 珊 张久顺 魏晓丽(475)
非负载镍基催化剂的加氢性能	袁胜华 郑进保 谭亚南 伊晓东 贾立山 方维平(482)
负载氧化铁凹凸棒石脱硫剂的制备及再生工艺	李 澜 赵秋萍 陈俊伊 魏国玉 王青宁(487)
尿素法合成甲苯-2,4-二氨基甲酸正丙酯反应	耿艳楼 方鸿刚 安华良 王桂荣 赵新强 王延吉(494)
二维中心切割气相色谱法测定汽油中有机含氧化合物和苯含量	张继东 魏宇锋 陈俊水 王文青 石 磊(501)
CO <sub>2</sub> 驱与 H <sub>2</sub> O 驱采出液中原油性质对比	陈 颖 张 磊 孙锐艳 梁宏宝 孙男男 孙露露(508)
疏水缔合聚丙烯酰胺的结构表征及其缔合作用	李芙蓉 曲彩霞 刘 坤 徐 辉 何冬月(513)
超细铜粉在合成润滑油 PAO10 中的摩擦学性能	张智宏 左晓亮 梁慧军(519)
3 株润滑油高效降解菌的降解性能	郭晓燕 王建军 何广湘 王 腾 李翠清(526)
三维电极体系中有有机物降解电流效率及动力学	乔启成 赵跃民 王立章 顾卫兵 杨春和(532)

### 综述

甲醇制芳烃研究进展	邹 琥 吴 巍 葱 雷 朱 宁 史军军(539)
-----------	--------------------------

### 信息

《石油学报(石油加工)》征订启事(408); 关于《石油学报(石油加工)》网上投稿的特别声明(452); 《China Petroleum Processing and Petrochemical Technology》征订启事(458); 《石油炼制与化工》征订启事(500); Ei 对中英文摘要的要求(512); 插图规范(548)

### \* 封面文章

期刊基本参数: CN11-2129/TE \* 1985 \* b \* A4 \* 180 \* zh+en \* P \* ¥20.00 \* 1500 \* 28 \* 2013-06 本期责任编辑: 白雪



# ACTA PETROLEI SINICA

## (PETROLEUM PROCESSING SECTION)

Vol. 29 No. 3 Jun. 2013

### CONTENTS

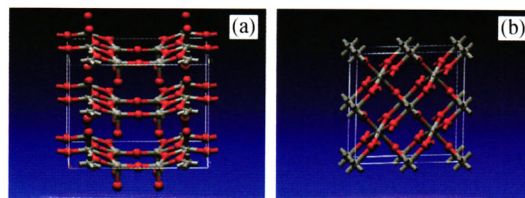
#### Research Articles

*Acta Petrolei Sinica (Petroleum Processing Section)*, 2013, 29(3): 369-375 doi: 10.3969/j.issn.1001-8719.2013.03.001

#### Effect of Lattice Oxygen of Vanadium Oxides on Thiophene Desulfurization

WANG Peng REN Kui TIAN Huiping LONG Jun

The desulfurization mechanism of thiophene over vanadium oxides was studied. It was found that the Lewis acid sites given by  $V^{n+}-O-V$  could be the initial adsorption site for thiophene, the synergetic effect of the said acid site and the adjacent  $V=O$  double bond could lead to the dissociation of  $C-S$  bond and the formation of  $CO$ ,  $SO_2$ ,  $H_2O$  and  $V-OH$  species.



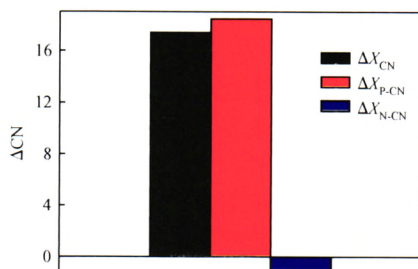
● Vanadium ● Oxygen  
(a)  $V_2O_5$  crystal; (b)  $VO_2$  crystal

*Acta Petrolei Sinica (Petroleum Processing Section)*, 2013, 29(3): 376-382 doi: 10.3969/j.issn.1001-8719.2013.03.002

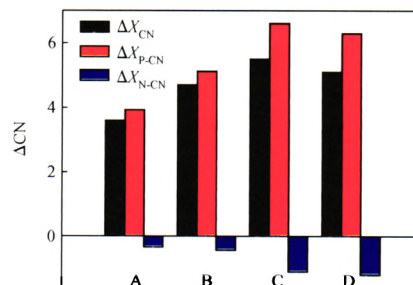
#### Relationship Between Hydrocarbons Reaction and Cetane Number in Diesel Hydro-Upgrading

ZHANG Yongkui HU Zhihai LIU Xiaoxin NIE Hong

The positive and negative contributions were 18.46 and 1.06 units, and the total cetane number due to the combination of positive and negative effects increased by 17.40 units in refining stage, while the positive and negative contribution were 3.93–6.60 and 0.33–1.19 units in the up-grading stage, and the final cetane number of up-grading product increased by 3.60–5.50 units over refining oil.



$\Delta X_{p,CN}$ —Positive contribution of aromatics hydrogenation saturation;  
 $\Delta X_{N,CN}$ —Negative contribution of cracking reaction of hydrocarbons with long side-chain;  $\Delta X_{CN}$ —Actual improvement of CN

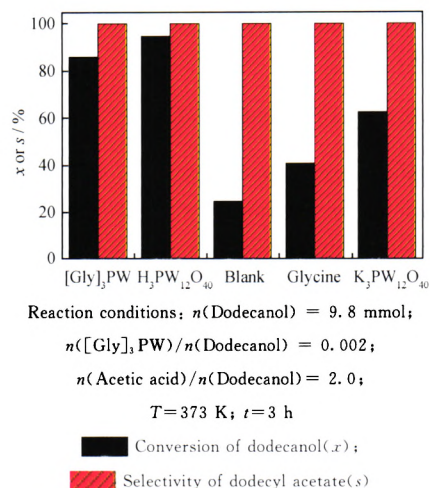


$\Delta X_{p,CN}$ —Positive effect of aromatics hydrogenation saturation and ring opening of cyclic hydrocarbons;  $\Delta X_{N,CN}$ —Negative effect in the cracking of side-chain of cyclic hydrocarbons;  $\Delta X_{CN}$ —Actual improvement of CN

### Preparation of Amino Acid Functionalized Heteropolyacid Salt and Its Catalytic Performance for Solvent-Free Esterification of Dodecanol With Acetic Acid

LIU Jing HUANG Xiaowen ZHAO Xiaoping LIU Xiumei  
YAN Peifang WANG Chang GAO Yan'an

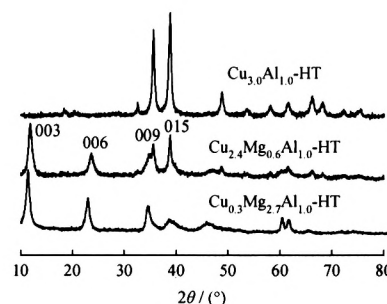
A new amino-acid functionalized heteropoly tungstates  $[\text{Gly}]_3\text{PW}$  was prepared via one-step synthesis method with glycine and phosphotungstic acid as raw materials. Its catalytic performance was investigated through the esterification of dodecanol with acetic acid. The good catalytic activity of  $[\text{Gly}]_3\text{PW}$  demonstrated that it was a very potential organic-inorganic hybrid catalyst.



### Highly Selective Catalytic Oxidation of Glycerol by Cu-Containing Hydrotalcites

LIU Xianfeng ZHANG Fang WANG Xiaoli DING Keqiang  
WANG Fang LIU Junhua SONG Xiaobo WU Gongde

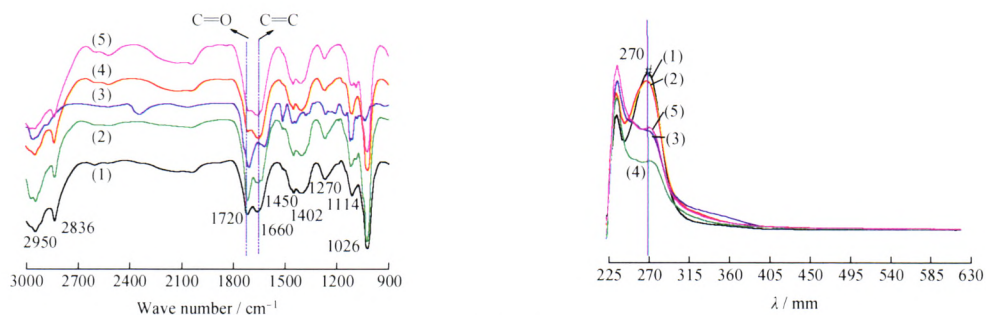
Cu-containing hydrotalcite catalysts ( $\text{Cu}_x\text{Mg}_y\text{Al}_z\text{-CHT-T}$ ) were synthesized and used in catalytic oxidation of glycerol. Among the prepared  $\text{Cu}_x\text{Mg}_y\text{Al}_z\text{-CHT-T}$  catalysts the  $\text{Cu}_{0.3}\text{Mg}_{2.7}\text{Al}_{1.0}\text{-CHT-450}$  possessed the highest catalytic performance for glycerol oxidation with glycerol conversion rate of 57.4% and glycolic acid selectivity of 73.7%.



### Upgradation of Light Fraction of Biomass Oil via Catalytic Hydrogenation

HU Enzhu XU Yufu LI Wendong LIU Tianxia HU Xianguo

The light fraction oil obtained from crude biomass oil could be catalytic hydrodeoxygenated over  $\text{MoS}_2$  catalyst at 150, 250, 350, 250/350°C and 2 MPa, respectively. The catalytic hydrodeoxygenation mechanism over  $\text{MoS}_2$  could be clarified via the unsaturated functional bonds ( $\text{C}=\text{C}$  and  $\text{C}=\text{O}$  sites) of the components in the light fraction oil that were easily attacked by the hydrogen during the proper temperature and pressure.

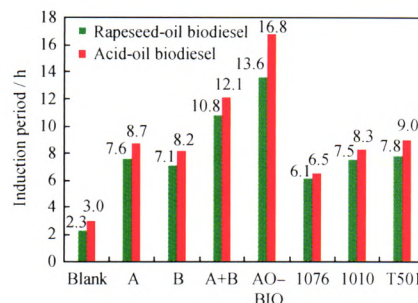


(1) Light oil;  
Upgraded oil,  $T/^\circ\text{C}$ : (2) 150; (3) 250; (4) 350; (5) 150/350

### Synthesis of Phenol-Amide Antioxidant AO-BIO and Its Application in Biodiesel

LIU Jinsheng LIN Jianmin ZHANG Jianrong ZHANG Yongguang

*N*-containing groups were introduced into methyl 3-(3,5-di-*tert*-butyl-4-hydroxyphenyl) propionate through the ester-to-amide reaction and antioxidant AO-BIO was obtained. The novel antioxidant AO-BIO showed better performances than other common phenolic antioxidants in the acid oil biodiesel, rapeseed oil biodiesel and biodiesel fuel blends tested by using Rancimat oxidation test method(EN 14112:2003 and EN 15751:2009).

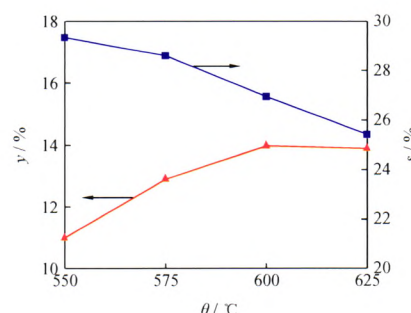


A—3,5-Methyl ester; B—*N*-aminoethyl piperazine; A+B—The complex of 3,5-methyl ester and *N*-aminoethyl piperazine with the mole ratio of 1

### Kinetic Modeling of Gasoline Catalytic Cracking to Propylene II. Model Analysis

LÜ Lufeng LI Bo HE Jinlong HOU Shuandi

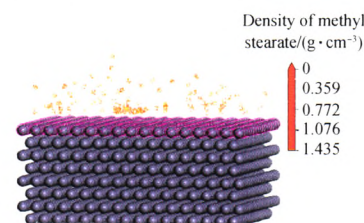
The effects of reaction temperature, catalyst/oil mass ratio and mass space velocity on the product distribution of FCC gasoline catalytic cracking performance were investigated by using a fixed-fluidized bed reactor. The kinetic model was analyzed by experimental results, showing that calculated results of cracking product distribution were well consistent with experimental data.



### Molecular Dynamics Simulation on the Adsorption Behavior of Biodiesel Components on Iron Surface

LUO Hui FAN Weiyu LI Yang NAN Guozhi

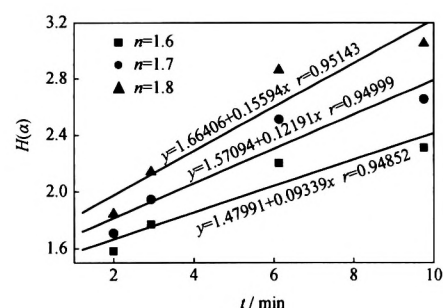
The adsorption behaviors of biodiesel components on Fe(110) surface were investigated by using molecular dynamics(MD) simulations. Biodiesel components could be adsorbed on the iron surface to form a hydrodynamic film and improve the lubricity of low-sulfur diesel. Double bonds or hydroxyl group introduced or an increase in the chain length could enhance the stability of the adsorbed films.



### Pyrolysis Kinetic Analysis for Water-soluble Fraction of Bio-oil in Fixed Bed Reactor

LIU Shaomin CHEN Mingqiang HU Qingsong  
YANG Zhonglian LI Feng WANG Juan WANG Jun

Thermodynamic parameters and the reaction order of water-soluble fraction of bio-oil were investigated. Fig.1 showed the relation of  $H(\alpha)$  and time at different reaction orders in the decomposition stage. The  $r$  values illustrated that the reactions were in well conformity with the corresponding reaction order.

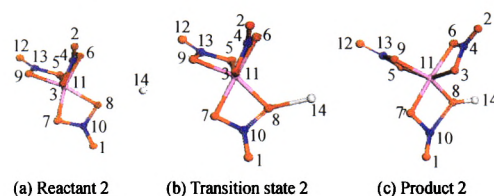




### Theoretical Study on Hydrogen Reduction of Nitrate

LI Qian GUO Dawei ZHOU Han

The mechanism of  $H_2$  reduction of  $Al(NO_3)_3$  was studied with density functional method. The reductions were performed by separated steps, such as formation of hydrogen radical, aluminum nitrite, aluminum hydroxide and nitrogen oxide followed by  $NO$  to  $N_2$ . The key step was dissociation of  $H_2$  into radicals.

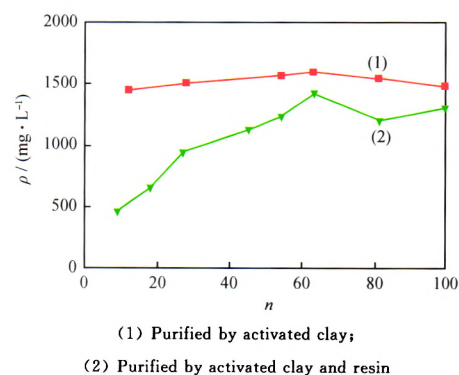


The reaction paths of reaction step of  $(NO_3)_2-Al-NO_3 + H \cdot \rightarrow (NO_3)_2-Al(NO_2)-OH$

### Purification of Lean Sulfolane by Using Clay and Resin Series Program

HAN Dong ZHANG Jimei LI Mingyu WEI Jun

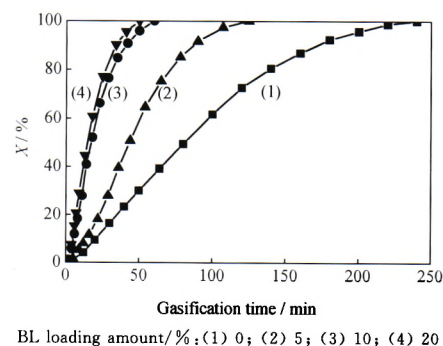
An activated clay and anion-exchange resin program of removing the colloid from lean sulfolane was proposed. The test results showed that the mass concentration of the colloid in lean sulfolane was decreased from 1800 mg/L to 900 mg/L after purification.



### Gasification Characteristics of Petroleum Coke Catalyzed by Black Liquor in a Fluidized Bed

YU Deping ZHANG Yuming YANG Yunquan GAO Shiqiu XU Guangwen

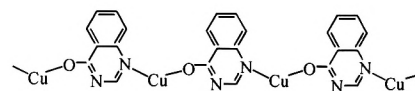
Black liquor (BL) could not only effectively improve the gasification reactivity in steam gasification of petroleum coke, but also greatly enhance  $H_2$  volume fraction in the produced syngas, which was an effective catalyst for petroleum coke gasification to produce  $H_2$ -rich syngas.



### Performance of Zero-Sulphur/Phosphorus Quinazolinone Amine as Multifunctional Lubricating Oil Additive

OUYANG Ping CHEN Guoxu ZHANG Xianming

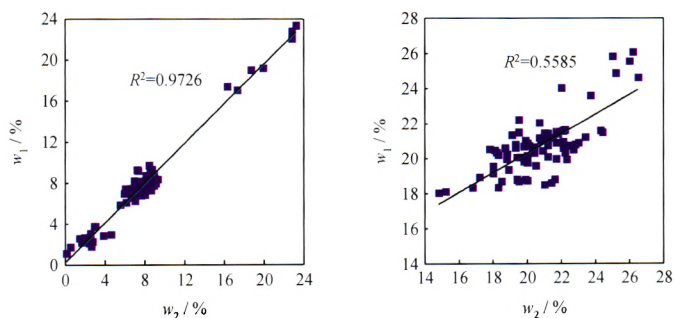
A new zero-sulphur/phosphorus lubricating oil additive of quinazolinone amine was investigated. It had good thermal stability with the extrapolated in cipient decomposing temperature up to  $240^\circ C$ , and the liquid paraffin with 1.0% of quinazolinone amine possessed excellent anti-corrosion and antirust characteristics with the antirust time over 168 h, which exceeded the value of the liquid paraffin with same amount of special antirust additive T746.



### Fast Determination of Gahnite Content in S Zorb Regenerated Sorbent by PLS-XRD

FU Ying ZHANG Xin ZOU Kang XU Guangtong

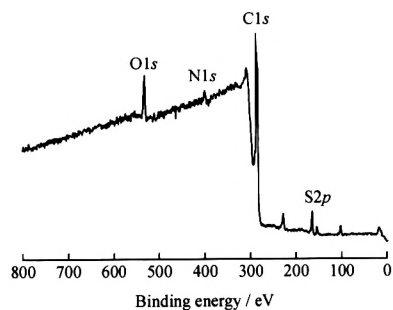
For fast determination of non-activated gahnite(zinc aluminate and Willemite) content in S Zorb regenerated sorbent, quantitative calibration models were first established by partial least square (PLS) regression based on the data of XRD combined with information from Rietveld quantitative phase analysis method.



### Study on XPS of Venezuela Heavy Oil Asphaltene

LI Chuan WANG Jiqian SUI Litao CUI Min DENG Wenan

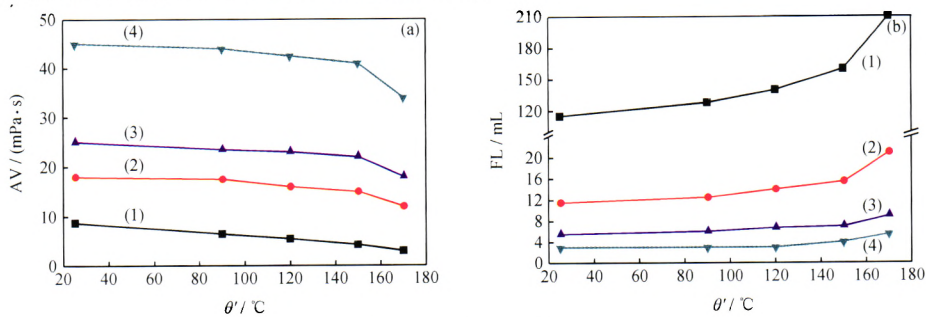
Functional groups on the surface of Venezuela heavy oil asphaltene were analyzed by XPS. Results showed that among hetero-atomic functional groups, carbonyl content was the most, contents of pyrrolic nitrogen and aliphatic sulfur were less than carbonyl, and contents of hydroxyl, carboxyl, pyridinic nitrogen and thiophenic sulfur were almost the same.



### Preparation and Properties of Heat- and Salt-Tolerant Viscosity Improver PADA in Water-Based Drilling Fluid

YAN Lili SUN Jinsheng WANG Jianhua WANG Chengbiao XU Bo YANG Zexing

With the increase of PADA concentration, the saturated salt-based mud system displayed a huge increase in apparent viscosity (AV) and a considerable decrease in filtrated loss (FL). The mud properties barely varied before and after aging tests, meaning that the mud formulations had excellent tolerance to salt and temperature.

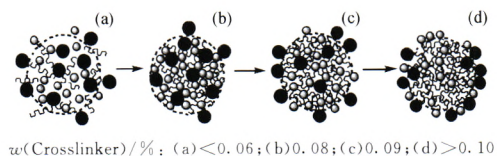


(a) Apparent viscosity; (b) Filtrate loss  
PADA adding amount/%: (1) 0; (2) 0.5; (3) 1.0; (4) 1.5

### Pore Diameter Adjustment of Sodium Polyacrylate and Balance Control of Selective Adsorption Property for Oil and Water

WU Yun ZHANG Xianming CHEN Bin CHEN Guoxu

In the schematic diagram of selective absorbing oil and water by polymer prepared with different amount crosslinker, it can be seen that when crosslinker amount was 0.09%, water/oil adsorption ratio of the polymer reached its highest value and the capability of selective adsorption was the strongest.

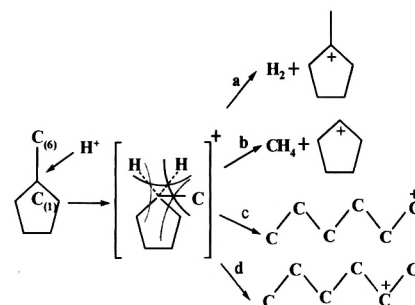


### Research Notes

### Exploration and Analysis on Ethylene and Propylene Formation in Naphthene Catalytic Cracking

YU Shan ZHANG Jiushun WEI Xiaoli

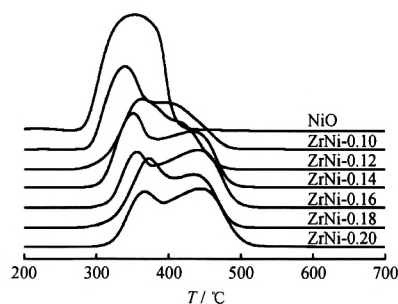
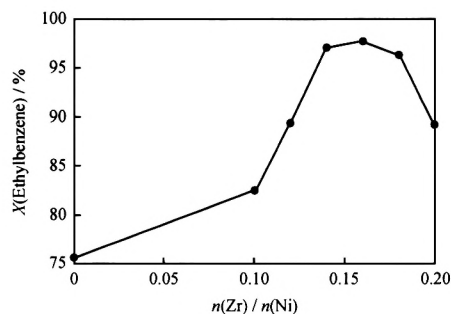
Based on the product distribution in methylcyclopentane catalytic cracking and molecular simulation results, it was supposed that  $H^+$  preferred to attack the carbon atom of methyl-substituent before charge transfer, forming  $C_{(1)}$  pentacoordinated carbocation.



### Hydrogenation Performance of Unsupported Ni-Based Catalyst

YUAN Shenghua ZHENG Jinbao TAN Ya'nan YI Xiaodong JIA Lishan FANG Weiping

Unsupported Ni-Zr catalysts, prepared by solid-phase-reaction method, possessed relatively large surface area. The Ni-Zr catalyst with suitable interaction of Ni and Zr exhibited a certain adsorption capacity for  $H_2$  and excellent ethylbenzene hydrogenation activity.

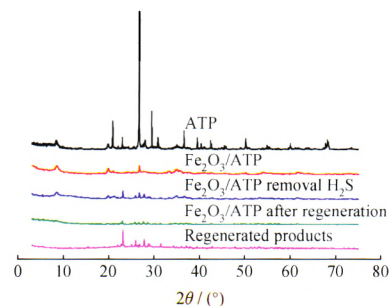




### Preparation of Iron Oxide Supported Attapulgite Desulfurizer and Its Regeneration Process

LI Lan ZHAO Qiuping CHEN Junyi WEI Guoyu WANG Qingning

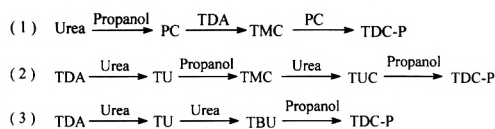
Fe<sub>2</sub>O<sub>3</sub>/ATP desulfurizer was prepared by impregnation method and was regenerated by heat air method. With the Fe<sub>2</sub>O<sub>3</sub>/ATP desulfurizer prepared under the optimal conditions, the sulfur capacity of 33.08% could be obtained for the removal of high concentration H<sub>2</sub>S, and as regenerated under the optimal conditions, the regeneration efficiency of Fe<sub>2</sub>O<sub>3</sub>/ATP reached 81.22%.



### Synthesis of Dipropyl Toluene-2,4-dicarbamate via Urea Route

GENG Yanlou FANG Honggang AN Hualiang WANG Guirong  
ZHAO Xinqiang WANG Yanji

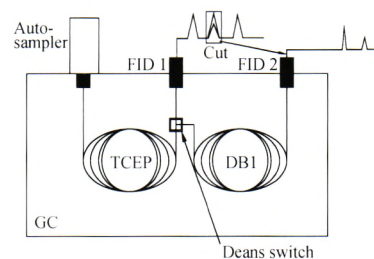
Dipropyl toluene-2,4-dicarbamate (TDC-P), with lower pyrolysis temperature than dimethyl toluene-2,4-dicarbamate to synthesize TDI, was synthesized successfully by using 2,4-diamino toluene (TDA), urea and propanol as raw materials in the absence of catalyst. TDA conversion, TDC-P yield and selectivity attained 95.3%, 66.1% and 69.4%, respectively. There existed three possible reaction paths for TDC-P synthesis.



### Determination of Organic Oxygenates and Benzene in Gasoline by Two-Dimensional Gas Chromatography With a Heart-Cutting System

ZHANG Jidong WEI Yufeng CHEN Junshui WANG Wenqing SHI Lei

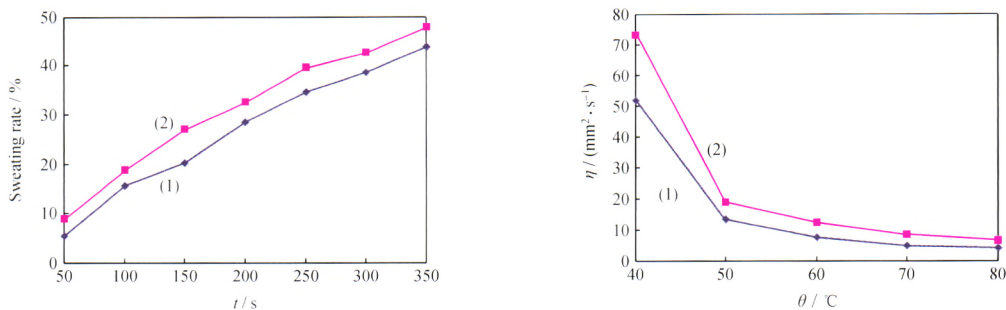
The contents of benzene and organic oxygenates in gasoline were determined by two-dimensional gas chromatography with a heart-cutting system. The retention time of common organic oxygenates and benzene in gasoline were confirmed both when column switched and non-switched, and a new dual-column qualitative and quantitative analysis method was established.



**Comparison on the Nature of the Crude Oil From CO<sub>2</sub> Flooding and H<sub>2</sub>O Flooding**

CHEN Ying ZHANG Lei SUN Ruiyan LIANG Hongbao SUN Nannan SUN Lulu

The article showed that the acid number and the content of resin and asphaltene of the crude oil from the CO<sub>2</sub> flooding produced fluid were more and the viscosity and the interfacial tension were lower than that of the one from H<sub>2</sub>O flooding.

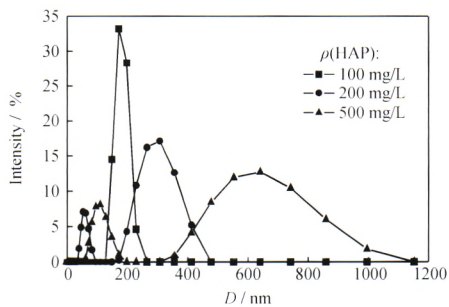


(1) CO<sub>2</sub> flooding; (2) H<sub>2</sub>O flooding

**Association and Structure Characterization of Hydrophobically Associating Polyacrylamide**

LI Meirong QU Caixia LIU Kun XU Hui HE Dongyue

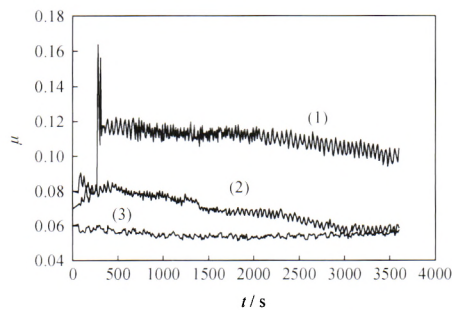
The measured CAC of HAP solution was in the range of 150–200 mg/L. When HAP mass concentration was 100 mg/L, there was a single peak in HAP particle size distribution and no network structure. A thin network structure and a double-peak distribution in particle size appeared at 200 mg/L of HAP mass concentration. The two peaks of particle size distribution shifted to right and the network structure was thicker at 500 mg/L of HAP mass concentration.



**Tribological Properties of Ultrafine Copper Particles in Synthetic Lubricant PAO10**

ZHANG Zhihong ZUO Xiaoliang LIANG Huijun

The friction coefficient of lubricating oil sample with ultrafine Cu particles was lower than the pure PAO10 in the entire friction process, and the excellent anti-friction function was obtained.



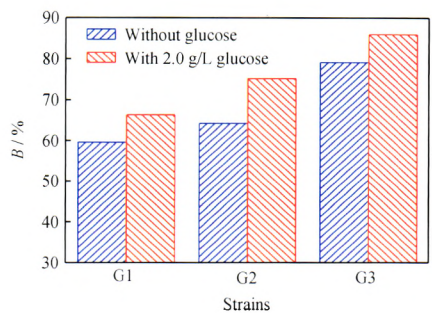
(1)PAO10;(2)PAO10+0.03% Cu-MPs;(3)PAO10+0.05% Cu-NPs



**Characteristics of Three Efficient Lube Oil Biodegrading Bacteria**

GUO Xiaoyan WANG Jianjun HE Guangxiang WANG Teng  
LI Cuiqing

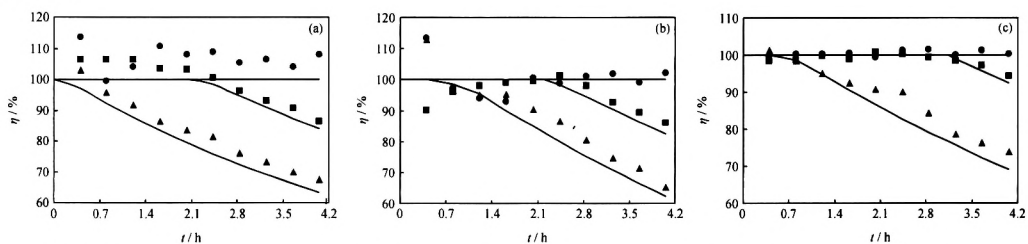
Three lube oil biodegrading strains were screened and identified as *Xanthomonas*, *Azotobacter* and *Pseudomonas*. Biodegradation characteristics such as pH value, temperature, inoculation concentration, initial oil volume, and glucose were studied. Under the appropriate conditions, the biodegradation capability of the three strains within 3 d was 66.4%, 75.3% and 86.1%, respectively.



**Current Efficiency and Kinetic Model for Degradation of Organic Compounds by Three Dimension Electrode System**

QIAO Qicheng ZHAO Yuemin WANG Lizhang GU Weibing YANG Chunhe

According to laws of indestructibility of matter and Farady, the description of current efficiency and kinetic model were evaluated in TDEs. Experimental results were in good agreement with the proposed equation, which could be used for the optimal design and manage of TDEs.



The solid lines represent the theoretical current efficiency. (a) DSD acid;  $i/(A \cdot m^{-2})$ : ●—5; ■—12; ▲—16; (b) Accelerator M<sub>1</sub>;  $i/(A \cdot m^{-2})$ : ●—20; ■—45; ▲—60; (c) Polyethylene polymerization initiator;  $i/(A \cdot m^{-2})$ : ●—80; ■—200; ▲—350

**Review**

**Review of Methanol to Aromatics**

ZOU Hu WU Wei XI Lei ZHU Ning SHI Junjun

Methanol to aromatics (MTA) process is a member of family of methanol to hydrocarbons (MTH) technologies. The review is focused on the industrial MTA drivers, MTA reaction mechanism, catalysts, processes, and further developments, especially the current status of the coal-based MTA technology in China.

